

ARTICLES

Structure and Dynamics of Polymer–Surfactant Complexes: Dielectric Relaxation Studies

Adalberto Bonincontro,[†] Paolo Michiotti,[‡] and Camillo La Mesa^{*‡}INFM-Department of Physics and Department of Chemistry, Università di Roma “La Sapienza”,
P.le A. Moro 5, 00185 Rome, Italy

Received: May 14, 2003; In Final Form: October 20, 2003

The isothermal phase diagram of the system composed of water, sodium dodecyl sulfate, and hexadecyltrimethylammonium polyacrylate, PACTA, at 25 °C, was investigated by dielectric relaxation, ionic conductivity, and viscosity. The polymer is not water-soluble and dissolves only in the presence of surfactant in micellar form. Dielectric relaxation spectra indicate the occurrence of one relaxation in the surfactant solutions, above the critical micellar concentration, and of two relaxation processes in the presence of PACTA and sodium dodecyl sulfate, $C_{12}SO_4Na$, in micellar form. They are ascribed to free and polymer-bound micelles, respectively. Data have been interpreted in terms of a chemical equilibrium of micelles partitioned between polymer-bound and free states. The dielectric results indicate that the distance between micelles adsorbed on the polymer backbone is close to 40 nm and slightly changes, depending on the surfactant content. These results support the hypothesis of a necklace structure for the polymer–micelle complex. According to viscosity findings, in fact, the stiffness of the PACTA- $C_{12}SO_4Na$ complex decreases on increasing the amount of bound micelles.

Introduction

Much interest is currently focused on the behavior of systems containing polymers and surfactants, in solution, gel, and solid forms.^{1,2} The reasons for so deep an interest arise from the potentialities of the aforementioned materials in practical applications.^{3,4} Their uses as viscosity modulators and adsorbent matrixes are more relevant.^{5,6} Other practical applications span from biomedical purposes⁷ to cosmetics and food sciences.⁸ Early studies on polymer–surfactant systems go back to the 1970s,^{9,10} and a comprehensive view of the complex peculiarities inherent to the above systems is still under development.^{11–14} polymer–surfactant systems, PSSs, include adducts and complexes formed by (a) surfactant binding onto hydrosoluble polymers;¹⁵ (b) interactions of block copolymers with surface active agents;¹⁶ (c) interaction complexes between proteins and surfactants;¹⁷ (d) binding of surface active agents onto hydrophobically modified polymers;¹⁸ and (e) surfactant binding onto polyelectrolytes, and so forth.

The physicochemical characterization of PSS has been performed by structural,¹⁹ rheological,²⁰ thermodynamic,²¹ and spectroscopic methods²² as well as by transport properties.^{23–25} Other physically relevant aspects, such as those inferred from dielectric methods, are not much investigated. Dielectric properties give almost unique information on the charge distribution in solid polymer–surfactant complexes,^{26,27} on the complex fluids they form, and on their polarization in solution. They may support the validity of models proposed for the organization of polymers and surfactants into complex structures.^{28,29} Comparison of dielectric properties with results obtained from other methods may clarify, in our opinion, still-open questions.

The present study deals with the interactions between a strongly hydrophobic polyelectrolyte, hexadecyltrimethylammonium polyacrylate, indicated as PACTA, and sodium dodecyl sulfate. PACTA was obtained by reacting poly(sodium acrylate) with equivalent amounts of a cationic surfactant.³⁰ The resulting product is formed by the invagination of polyacrylate chains in a compact, tubular pocket consisting of many hydrocarbon chains, with the apolar groups facing outward. Physically, adsorption of a surfactant monolayer onto a linear polyelectrolyte occurs. The structure of PACTA, obtained by X-ray diffraction,^{31,32} is similar to that inferred by small-angle X-ray scattering on structurally related polymer–surfactant complexes.³³ PACTA is not water soluble but is dissolved in the presence of surfactants in micellar form. The purpose of this contribution is to clarify the surfactant-assisted solubilization of PACTA, to focus on the forces responsible for dissolution, and to forecast a reasonable hypothesis for the role of micelles in the solubilization mechanism. We present a model for the structure of the supercolloidal objects obtained by mixing PACTA and SDS in water and compare it with the flexible rod,³⁴ or the necklace,³⁵ ones. The observed behavior has structural analogies with those occurring in complex colloidal structures, including those observed in protein–surfactant systems.^{36,37}

Experimental Section

Materials. Sodium dodecyl sulfate, $C_{12}SO_4Na$, polyacrylic acid (average molecular masses of 2.0 and 250 kD, respectively), sodium hydroxide, hexadecyltrimethylammonium bromide, indicated as $C_{16}NMe_3Br$, butan-2-ol, and other reagents were from Aldrich.

Water was deionized and distilled over alkaline $KMnO_4$. Its ionic conductivity, χ , is close to $1 \mu S m^{-1}$, at room temperature.

$C_{12}SO_4Na$ was dissolved in hot ethanol; the resulting solution was filtered, to remove dust or other particles, cooled, and

* Corresponding author. E-mail address: camillo.lamesa@uniroma1.it.

[†] INFM-Department of Physics, Università di Roma.

[‡] Department of Chemistry, Università di Roma.

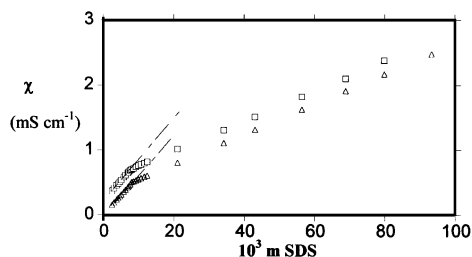


Figure 1. Specific conductance, κ , in $(\Omega \text{ cm})^{-1}$, of $\text{C}_{12}\text{SO}_4\text{Na}$ in water (triangles) and in 1.00 wt % PACTA solution (squares) at 25 °C. To avoid overlapping, double scales have been reported on the left- and right-hand sides of the figure. The dotted lines indicate the conductivity behavior below the cmc.

precipitated by acetone. The solid was vacuum-dried at 70 °C, for 2 days. Its critical micellar concentration (cmc), obtained by conductivity, is 8.2 mmol kg^{-1} , at 25 °C.^{38,39}

The preparation of PACTA is a modification of formerly reported procedures.^{30–32} About 160 mL of $\text{NaOH } 1 \times 10^{-2} \text{ mol dm}^{-3}$ were added to 10 g of PAH in 200 mL of water, at 40 °C. The poly(sodium acrylate) solution was filtered and reacted with aqueous $\text{C}_{16}\text{NMe}_3\text{Br}$, under stirring, at 40 °C. The titration was controlled by conductivity and optical methods. The maximum turbidity occurs at complete charge neutralization of the polyelectrolyte. Ionic conductivity, conversely, changes in slope once the titration of poly(sodium acrylate) by $\text{C}_{16}\text{NMe}_3\text{Br}$ is completed. The cloudy dispersion obtained by complete titration was centrifuged (6000 rpm), and the precipitate was twice extracted with butan-2-ol. The organic solution was distilled under a reduced pressure, and the residue was vacuum-dried at 70 °C. More details on the synthetic and purification procedures are given elsewhere.^{31,32}

The mass of PACTA, inferred by HPLC, is about $1.2 \pm 0.1 \times 10^6 \text{ D}$, corresponding to an almost complete titration of poly(sodium acrylate) by the cationic surfactant. In agreement with findings relative to structurally related systems,^{40,41} the PACTA solubility in water is extremely low. This is a further indication of an almost complete charge neutralization. PACTA contains 3400 ± 300 acrylate units. Assuming the distance between adjacent COO^- units to be 0.4 nm, its chain length in the fully extended conformation is estimated to be $1.2 \pm 0.1 \mu\text{m}$ long.

Methods. Electrical Conductivity. A Wayne-Kerr bridge, model 6425, was used. The cell is located in an oil bath, at 25.000 ± 0.002 °C. The temperature, T , was measured by a platinum thermometer, with an accuracy of 0.001 °C. Ionic conductivity data are reported in Figure 1.

Phase Diagram. The samples were prepared by weight in glass vials, which were flame sealed, heated 2 days at 50 °C, and equilibrated at 25 ± 1 °C for 1 week. Studies refer to the dilute regime, below 4 wt % complex. In multiphase systems, long times are required to reach thermodynamic stability (several months). The partial phase diagram of the system water–PACTA– $\text{C}_{12}\text{SO}_4\text{Na}$ is reported in Figure 2.

Solution Viscosity. Ubbelohde-type viscometers, Schott, having flow times in the range 2–300 s, were used. Measurements were performed at 25.00 ± 0.01 °C in a water bath. The temperature was controlled to ± 0.001 °C by an F25 thermometer, A.S.L. At least five independent runs were performed for each point, and the uncertainty of the flow times is less than 0.3 s. The relative viscosity, η_{rel} , was obtained by

$$\eta_{\text{rel}} = \eta/\eta^\circ = t\rho/t^\circ\rho^\circ \quad (1)$$

where t and t° are the flow times of the solution and the solvent,

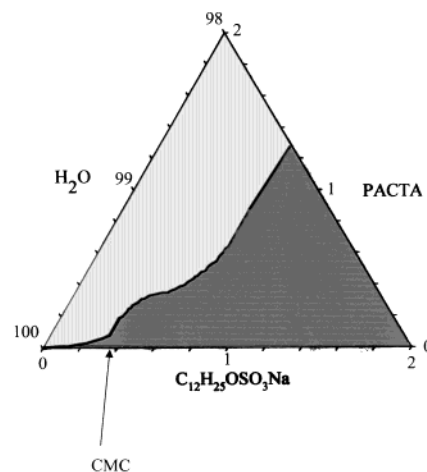


Figure 2. Partial phase diagram of the system water– $\text{C}_{12}\text{SO}_4\text{Na}$ –PACTA, at 25 °C. The light gray area indicates a two-phase region containing water, surfactant, and nondissolved polymer. The arrow in the bottom indicates the cmc of the pure surfactant.

respectively, and ρ and ρ° are the solution and solvent densities. Selected viscosity data are reported in Figure 3.

Densities, ρ , were determined by a DMA 60 Anton Paar vibration densimeter, at 25.000 ± 0.002 °C. A digital thermometer measured the temperature, T . Densities were obtained by

$$\Delta\rho = \rho - \rho^\circ = (1/A)(\tau^2 - \tau^{\circ 2}) \quad (2)$$

where τ° and τ are the vibration frequencies of the measuring cell with the solvent and the solution, respectively. The A constant was obtained by fitting eq 2 for water,⁴² acetone, ethanol, and ethylene glycol.⁴³ The accuracy of the ρ values is $5 \times 10^{-6} \text{ g cm}^{-3}$.

Dielectric Relaxation. The permittivity, ϵ' , and dielectric loss, ϵ'' , were measured by computer-controlled Hewlett-Packard impedance analyzers, models 4194-A and 4291-A, respectively, in the range 10^5 – 10^9 Hz. The measuring cell, previously described,⁴⁴ is a section of a cylindrical waveguide filled with the solution. The whole system behaves as a waveguide excited far beyond its cutoff frequency mode, and only the stray field of the [coaxial line/waveguide] transition is used. The cell constants were determined by measuring the dielectric response of electrolyte solutions of known conductivity.⁴⁵ The errors on ϵ' and ϵ'' are within $\pm 1\%$. The temperature was stabilized to 25.0 ± 0.1 °C by an external liquid circulation bath.

The best fit to the experimental dielectric relaxation spectra was obtained by combining, up to convergence, the plots of ϵ' versus $\log f$, ϵ'' versus $\log f$ (in MHz), and ϵ' versus ϵ'' into Cole–Cole plots. The accuracy of the relaxation times and amplitudes is to a few percent. The best fit curves are indicated in Figures 4–7 as full lines.

Results

Dielectric Measurements. The dielectric properties of the single components in solution, that is, the behavior of the $\text{C}_{12}\text{SO}_4\text{Na}$ –water system, the $\text{C}_{16}\text{NMe}_3\text{Br}$ –water one, and the sodium polyacrylate (PANa)–water mixtures, have been investigated. No electrolytes were added to the water–surfactant mixtures, to the water poly(sodium acrylate), or to the water–PACTA– $\text{C}_{12}\text{SO}_4\text{Na}$ ones. The preliminary investigation quantifies separately the contributions of the different surfactants and of the polyelectrolyte to the dielectric response of the mixtures.

The behavior of sodium dodecyl sulfate micellar solutions was studied by measuring the complex permittivity in the range

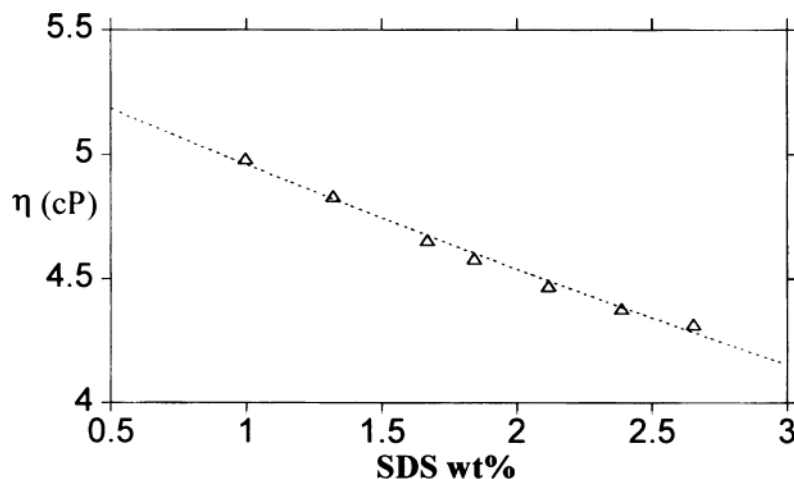


Figure 3. Dependence of the absolute viscosity, in cP, on added $\text{C}_{12}\text{SO}_4\text{Na}$, at 25 °C. The mother solution contains 1.06 wt % $\text{C}_{12}\text{H}_{25}\text{SO}_4\text{Na}$ and 1.02 wt % PACTA.

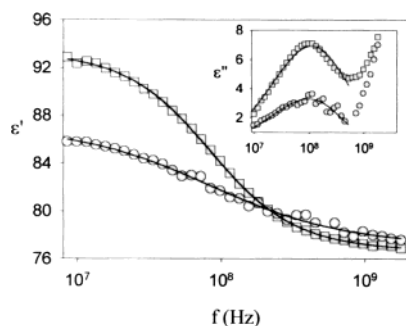


Figure 4. Real part of the dielectric relaxation spectrum, ϵ' , versus $\log f$ (in Hz) relative to $3.1 \times 10^{-2} \text{ m}$ $\text{C}_{12}\text{SO}_4\text{Na}$ (squares) and to $2.0 \times 10^{-2} \text{ m}$ $\text{C}_{16}\text{NMe}_3\text{Br}$ (circles), at 25 °C. In the inset are reported the corresponding imaginary components, ϵ'' . The solvent relaxation, at high frequencies, is evident. Here and in the following the solid lines indicate the best fits of data.

TABLE 1: Surfactant Molal Concentration, Relaxation Frequency, f^* , and Amplitude, $\Delta\epsilon$, of Solutions Containing $\text{C}_{12}\text{SO}_4\text{Na}$, $\text{C}_{16}\text{NMe}_3\text{Br}$, or Their Mixtures, at 25 °C^a

surfactant	molal concentration (<i>m</i>)	f^* (MHz)	$\Delta\epsilon$
$\text{C}_{12}\text{SO}_4\text{Na}$	$3.1 \times 10^{-2} (\pm 0.1)$	50 (± 2)	3.7 (± 0.1)
$\text{C}_{12}\text{SO}_4\text{Na}$	$1.70 \times 10^{-1} (\pm 0.01)$	84 (± 2)	17.5 (± 0.3)
$\text{C}_{16}\text{NMe}_3\text{Br}$	$2.0 \times 10^{-2} (\pm 0.1)$	75 (± 3)	8.4 (± 0.3)
$\text{C}_{16}\text{NMe}_3\text{Br} + \text{C}_{12}\text{SO}_4\text{Na}$	$2.4 \times 10^{-2} + 11.0 \times 10^{-2} (\pm 0.1)$	29 (± 1)	46 (± 1)

^a Errors are given in parentheses.

1 MHz–1 GHz. In Figure 4, the real and imaginary components of the dielectric permittivity for an aqueous $\text{C}_{12}\text{SO}_4\text{Na}$ solution are reported. A single relaxation process is evident. The dielectric increment, $\Delta\epsilon$, and the relaxation frequency, f^* , Table 1, depend on concentration. They are close to those formerly reported by Barchini and Pottel.⁴⁶ In Figure 4 is also reported the dielectric response of an aqueous $\text{C}_{16}\text{NMe}_3\text{Br}$ solution, in the same frequency range. A dielectric dispersion similar to that observed in sodium $\text{C}_{12}\text{SO}_4\text{Na}$ is evident. Accordingly, the mechanism underlying the dielectric relaxation in ionic surfactant solutions is the same, irrespective of the net charge of micelles and counterions. Similar findings, used in modeling the distribution of counterions around ionic surfactant micelles, have been formerly reported in the literature.^{46–50}

To put in evidence the dielectric dispersion of the polyelectrolyte, the permittivity of PANa in solution was measured. Two

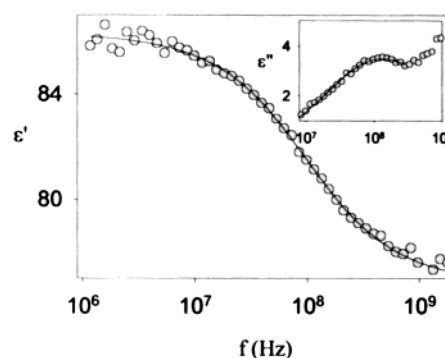


Figure 5. Real, ϵ' , and imaginary, ϵ'' , components of the dielectric relaxation spectrum relative to a $2.1 \times 10^{-3} \text{ m}$ PANa solution, at 25 °C, as a function of $\log f$ (Hz). The molar mass of the polyelectrolyte is $2.7 \times 10^3 \text{ D}$. A similar behavior has also been observed in high-molecular-weight poly(sodium acrylates).

TABLE 2: Polymer Concentration, Relaxation Frequency, f^* , and Amplitude, $\Delta\epsilon$, of Mixtures Containing PANa of Different Molecular Weights, at 25 °C^a

polymer	molal concentration (<i>m</i>)	f^* (MHz)	$\Delta\epsilon$
PANa 2.7 kD	$2.1 \times 10^{-3} (\pm 0.1)$	213 (± 5)	10.8 (± 0.8)
PANa 330 kD	$5.1 \times 10^{-4} (\pm 0.1)$	260 (± 20)	15 (± 2)

^a Errors are given in parentheses.

different molecular weight polymers, having molar masses of 2.0×10^3 and $2.5 \times 10^5 \text{ D}$, respectively, were investigated. In both cases, the behavior typical of linear polyelectrolytes was observed.^{51,52} In both systems, the relaxation frequencies in Figure 5 are well above 100 MHz. The relaxation parameters, reported in Table 2, are consistent with affirmed models for polymer chain flexibility.^{53,54}

Samples containing proper amounts of $\text{C}_{12}\text{SO}_4\text{Na}$ and $\text{C}_{16}\text{NMe}_3\text{Br}$ were investigated. The concentrations simulate the conditions that could occur whenever PACTA completely dissociated in ions and mixed aggregates, containing both cationic and anionic surfactants, was formed. Catanionic mixtures are formed, for instance, by mixing $\text{C}_{12}\text{SO}_4\text{Na}$ and $\text{C}_{16}\text{NMe}_3\text{Br}$ surfactants. The cmc of catanionic mixtures is much lower than the ones of the pure components,⁵⁵ and the solution contains electrolyte in excess. The 1-1 mixtures are poorly water-soluble:⁵⁶ a slight excess of one surfactant leads to the formation of mixed micelles, or vesicles.^{8,57} The

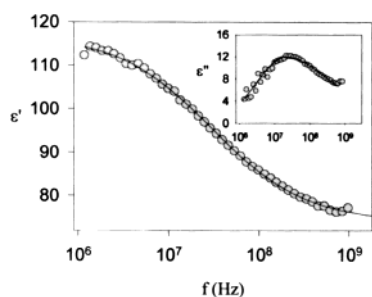


Figure 6. Real, ϵ' , and imaginary, ϵ'' , components of the dielectric relaxation spectrum as a function of $\log f$ (in Hz) of a mixture containing $2.4 \times 10^{-2} m$ $C_{16}NMe_3Br$ and $1.1 \times 10^{-1} m$ $C_{12}SO_4Na$, at 25 °C. Higher ratios between the two components shift the relaxation frequency to lower values.

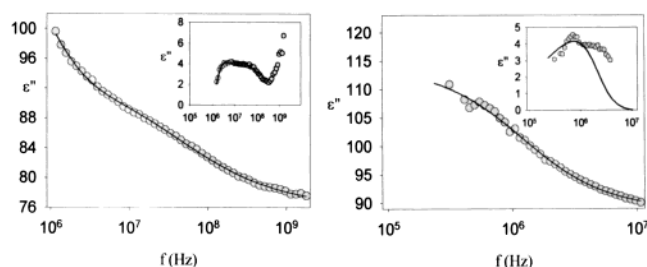


Figure 7. (a) Real, ϵ' , and imaginary, ϵ'' , components of the dielectric relaxation spectrum as a function of $\log f$ (in Hz) for mixtures containing $1.5 \times 10^{-6} m$ PACTA and $3.1 \times 10^{-2} m$ $C_{12}SO_4Na$, at 25 °C. (b) Real, ϵ' , component of the relaxation spectrum as a function of $\log f$ (in Hz) in the range 100 kHz–100 MHz.

TABLE 3: Polymer Concentration, Fast, f^*_f , and Slow, f^*_s , Relaxation Frequencies, and Related Amplitudes, $\Delta\epsilon$, of Mixtures Containing Different Amounts of PACTA in $3.1 \times 10^{-2} m$ $C_{12}SO_4Na$, at 25 °C^a

PACTA (μm)	f^*_f	$\Delta\epsilon_f$	f^*_s	$\Delta\epsilon_s$
1.5 (± 0.1)	44 (± 1)	5.9 (± 0.2)	1.32 (± 0.05)	8.2 (± 0.2)
5.2 (± 0.1)	43 (± 2)	19 (± 2)	1.04 (± 0.03)	13 (± 1)

^a Errors are given in parentheses.

experimental results for these mixtures (Figure 6) show a dielectric dispersion at a much lower frequency than $C_{12}SO_4Na$ or $C_{16}NMe_3Br$.

The dielectric spectra of a ternary system containing water, PACTA, and $C_{12}SO_4Na$ are reported in Figure 7a,b. Two partially overlapping relaxation processes, in the MHz region and around 40–50 MHz, respectively, are observed. Extending the measuring range to 10^5 Hz (Figure 7b) allows a much better definition of the low-frequency dispersion mode. The relaxation parameters do not depend significantly on concentration (Table 3).

Electrical Conductivity. Measurements were performed on $C_{12}SO_4Na$ solutions, to determine micelle formation and counterion binding and to evaluate the role of PACTA in the association features of the surfactant. According to Figure 1, there is no significant difference in surfactant association with or without PACTA. Presence of the polymer implies a small shift of the cmc values to a higher concentration. Addition of the hydrophobic polyelectrolyte does not influence ion transport, as indicated by the conductance behavior above the cmc. Micelle formation is concomitant to a significant decrease in the solution turbidity and to a complete dissolution of PACTA. The above effects are reversible upon dilution with water and suggest a negligible dissociation of PACTA.

Solution Viscosity. As a consequence of the poor solubility of PACTA, measurements were performed in micellar solutions, when the polymer dissolution is complete. Data in Figure 3 indicate that addition of $C_{12}SO_4Na$ is concomitant to a significant decrease of viscosity, η . The aforementioned behavior slightly depends on the PACTA wt % in the mixture.

Discussion

Our aim is to identify the interactions leading to the solubilization of PACTA in micellar solutions and to rationalize the role of electrostatic or hydrophobic contributions in such a process. Preliminary measurements were performed to determine the dielectric contributions due to the different mixture components and to predict how they are influenced by concentration. They are individually discussed in the following sections.

Micellar Solutions. An approach to account for the dielectric properties of micellar systems was originally developed by Grosse and Foster^{58,59} and was recently revised and slightly modified by other authors.^{46–50} In Grosse's theory, micelles are considered spheres of radius r with charges uniformly distributed on the surface. Micellar systems show dielectric relaxation processes in the radio-frequency range. The relaxation process is due to the diffusive phenomena of counterions adjacent to the (charged) micellar surface and depends on the surfactant content.

Two possible counterion diffusion processes are associated with micelle formation. The radial diffusion mode produces a polarization relaxing in the 10–100 MHz range. The second, due to a tangential motion of counterions along the micelle surface, is concomitant with relaxation processes in the 100–MHz range. The relaxation processes observed in Figure 4, hence, are essentially due to radial diffusion modes. The relaxation frequency, f^* , can be related to the micelle radius, r , according to⁵⁹

$$f^* = D/r^2 \quad (3)$$

where D is the diffusion coefficient of the counterions. By assuming D to be $1.33 \times 10^{-9} m^2 s^{-1}$ for Na^+ and $2.08 \times 10^{-9} m^2 s^{-1}$ for the Br^- ion, respectively,^{60,61} the radii of both the $C_{12}SO_4Na$ and the $C_{16}NMe_3Br$ micelles were calculated. The resulting values, 4.7 and 5.3 nm, respectively,⁶² are reasonable. Unexpectedly, the radius at high $C_{12}SO_4Na$ content is lower than that at low concentrations. Such a discrepancy implies effects not considered in the model. Presumably, the measured radius refers to charged spheres surrounded by an ion cloud, that is, the radius of the micelles plus the Debye screening length (which is inversely proportional to concentration).

Comparison with literature data indicates that the available micelle sizes⁶³ are lower than those obtained by dielectric relaxation. It must be pointed out, in this regard, that such data are obtained by scattering methods, when the present ones also account for the diffuse double layer around the micelles. To get reasonable values, thus, cogent hypotheses on the double layer thickness (i.e., the Debye screening length) must be considered. The Debye screening length, κ , is defined according to the equation⁶⁴

$$\kappa^2 = (10^3 e^2 N_A / \epsilon k T) \sum n_i z_i^2 \quad (4)$$

where ϵ is the solution permittivity, N_A is Avogadro's number, and the meanings of the other symbols are as usual. The term under the summation in eq 4 is twice the medium ionic strength. Let us introduce in the above relation a two-component model for micelle formation. Above the cmc, we assume the follow-

ing: (a) The concentration of free dodecyl sulfate ions equals the cmc. (b) Charged micelles contain, on average, $\langle N \rangle$ surfactant ions. The micelle charge is $\langle N \rangle - m$. (c) The concentration of free sodium ions corresponds to the cmc plus the amount of free ions dissociated from the micelles. Hence, the amount of free counterions is proportional to $m/\langle N \rangle$.

In words, the micellar system behaves as a mixture of two electrolytes: the surfactant in molecular form (dodecyl sulfate and sodium ions, at $C = \text{cmc}$) and a polyion, consisting of partially charged micelles. A similar approximation was proposed to quantify counterion binding to micelles⁶⁵ and, more recently, to rationalize the conductivity behavior in micellar solutions.⁶⁶ The medium ionic strength, I , can be expressed as

$$I = (1/2) \sum c_i z_i^2 = (1/2) \{ 2\text{cmc} + [(C_{\text{tot}} - \text{cmc})/\langle N \rangle] [\langle N \rangle - m]^2 + (m) \} \quad (5)$$

Combination with eq 4 gives

$$\kappa^2 = (10^3 e^2 N_A / \epsilon kT) \{ 2\text{cmc} + [(C_{\text{tot}} - \text{cmc})/\langle N \rangle] [\langle N \rangle - m]^2 + (m) \} \quad (6)$$

where $\langle N \rangle$ is close to 60⁶⁷ and the micelle fractional charge (the ratio $m/\langle N \rangle$) is about 0.4.⁶⁸ Taking into account $\langle N \rangle$ and the fractional charge of the micelles, reported in eq 6, the calculations indicate a Debye length in the range 2–3 nm in the concentration region we have investigated. Once the thickness of the double layer is obtained, it is possible to estimate the micelle radius. The combination of r values obtained from dielectric relaxation with the Debye screening length, calculated by eq 6, gives micelle radii very close to those obtained from light scattering experiments.⁶⁹

Mixed Micellar Systems. The dielectric results relative to samples containing both $\text{C}_{12}\text{SO}_4\text{Na}$ and $\text{C}_{16}\text{NMe}_3\text{Br}$, reported in Figure 6, show a dielectric dispersion at frequencies much lower than the single micellar species. In the charged sphere model for micelle formation, lower relaxation frequencies imply a larger size of the ion cloud. The observed effect, thus, is presumably related to the formation of mixed micelles with a low surface charge density as a result of (a) a partial neutralization of the charges relative to dodecyl sulfate ions by hexadecyltrimethylammonium ones and (b) an increase in micelle size. We do not know, at the present stage, whether aggregates formed by mixing $\text{C}_{12}\text{SO}_4\text{Na}$ and $\text{C}_{16}\text{NMe}_3\text{Br}$ are spherical, anisometric, or catanionic vesicles.⁵⁷

Polyelectrolytes. In PANa solutions, the relaxation frequency is high (≈ 260 MHz), Figure 5. The observed behavior can be interpreted in terms of classical models for the dielectric properties of polyelectrolyte solutions^{51–54} as a result of the motion of counterions along the polymer backbone. The dielectric behavior, thus, gives information on the physical features of the macromolecule.⁷⁰

In current models, the polymer is represented by a sequence of linear subunits of length b . For long enough macromolecules, b values are independent of the molecular weight. Counterions can freely move along each subunit but cannot pass to another. The latter possibility occurs if the potential barrier at the junction between each subunit is overcome.

In presence of external electric fields, the distribution of counterions is perturbed and an induced dipole moment is generated. Two relaxation processes, due to the induced polarization, may be observed in the radio-frequency range. The low-frequency dispersion (in the kHz region) is due to counterions travelling along the whole polymer chain. The second

dispersion (in the MHz region) is ascribed to counterions trapped in the same subunit. The equation for the induced polarization dispersion is

$$f^* = \pi k T u / 2b^2 \quad (7)$$

where u is the mobility of the counterions moving along a subunit of length b , f^* is the relaxation frequency, and k is the Boltzmann constant. The relaxation amplitude, $\Delta\epsilon$, is expressed as

$$\Delta\epsilon = e^2 F N C \gamma b^2 / 36 k T \epsilon_0 \quad (8)$$

where N is the number of charged sites per polymer chain, e is the counterion charge, C is the macromolecule concentration, in mol/m^3 , F is the fraction of bound counterions, γ (≈ 1 for dilute solutions) is the ratio between the actual electric field acting on the polyion and the average Maxwell field in solution, and ϵ_0 is the dielectric constant in a vacuum.

Equation 7 gives a b value that is about 3-nm long. The calculation was made assuming that the u parameter in eq 7 is the mobility of Na^+ ions at infinite dilution ($u \approx 3 \times 10^{11} \text{ m s}^{-1} \text{ N}^{-1}$).⁷¹ The estimated b value fits very well with the one inferred by eq 8 if the amount of bound counterions, F , is close to 0.54. The latter quantity can be deduced from activity measurements with a sodium selective electrode.^{53,54}

Polymer–Surfactant Complexes. Finally, the behavior of samples containing PACTA dissolved in $\text{C}_{12}\text{SO}_4\text{Na}$ micellar solutions was investigated. The concentrations were properly chosen to have homogeneous solutions. The dielectric measurements reported in Figure 7a put in evidence the presence of, at least, two different relaxation processes.

Two different solubilization mechanisms may occur: a dissolution-based and an adsorption-based one, respectively. In the former, the complete dissociation of PACTA is supposed. The hydrophobic pocket covering the polyacrylate moieties is dissolved, with consequent release of $\text{C}_{16}\text{NMe}_3$ ions and formation of mixed micelles with $\text{C}_{12}\text{SO}_4\text{Na}$. As a consequence of the above process, polyacrylate and mixed micelles will be present in solution. From a dielectric viewpoint, this hypothesis implies the occurrence of two relaxation processes, one in the MHz range (ascribed to the presence of mixed micelles) and a second centered at 200 MHz (due to polyacrylate). This hypothesis is not consistent with experiments. Ionic conductivity data, in addition, indicate that PACTA dissolution by $\text{C}_{12}\text{SO}_4\text{Na}$ does not imply changes in ion transport properties compared to pure sodium dodecyl sulfate.

Alternatively, we assume the polymer dissolution to be essentially micelle-assisted, that is, due to micelle adsorption onto the hydrophobic moieties of PACTA. Implicit in the hypothesis is the occurrence of a chemical equilibrium between polymer-bound and free micelles, in good agreement with the fact that polymer dissolution occurs above the cmc (Figure 2).

On thermodynamic grounds, the following relation can be introduced:



In terms of the dielectric behavior, this hypothesis implies the occurrence of (a) dielectric dispersions having a relaxation time close to that of free micelles (in the range 10–100 MHz) and (b) low-frequency dispersion modes, due to the interactions between the ion clouds of polymer-adsorbed micelles.

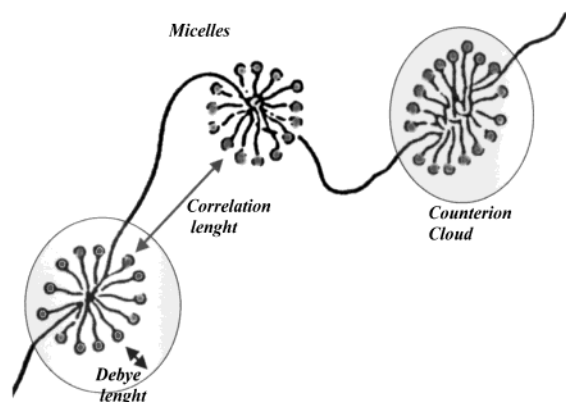


Figure 8. Necklace model for the formation of polymer–surfactant complexes. Empty circles indicate the counterion clouds. The Debye length is indicated too.

The low-frequency vibration modes are reasonably due to the presence of free segments on the polymer chain, located between two adjacent adsorbed micelles. The application of Mandel's relation^{53,54} to the low-frequency relaxation mode allows estimation of the correlation distance between charged micelles adsorbed on the polymer backbone. From a dielectric viewpoint, the complex can be considered a string onto which charged micelles are adsorbed. The distance between charged groups, b , is that between two micelles adsorbed onto the polymer. Calculations indicate b values to be about 40 nm and the number of bound micelles close to 25–30. In terms of chemical equilibrium, about 10% of the micelles are polymer-bound.

The best fit to the data in Figure 7a,b indicates the occurrence of two relaxation processes centered at 1 MHz and 40–45 MHz, respectively (Table 3). Within the limits set up by the fitting procedures, the amplitude and frequency of the second process are equivalent to those formerly found in free micelles.

Experimental evidence supports the second hypothesis. The ionic conductance is nearly the same in the ternary system and in pure $C_{12}SO_4Na$; that is, bound micelles are few compared to free ones. The amplitude of dielectric dispersion due to micelle formation is close to that observed in free micelles at the same concentration. Finally, data in Figure 3 indicate a slight, but significant, decrease of the solution viscosity upon addition of $C_{12}SO_4Na$. In words, the addition of the surfactant reduces the polymer chain stiffness, as a consequence of a reduced distance between micelles adsorbed on the polymer backbone.

The interactions between $C_{12}SO_4Na$ and PANa do not involve any sort of precipitate or interaction between the components, and the dielectric behavior of their mixtures can be considered in analogy to the overlapping of two (nearly) noninteracting colloidal solutes.

Conclusions

Information arising from the phase diagram, ionic conductance, viscosity, and dielectric relaxation experiments indicates the occurrence of interactions between micelles and PACTA. According to experimental evidence, micelle binding onto the polymer is controlled by a chemical equilibrium. As a consequence of this equilibrium, the presence of relaxation processes relative to free and polymer-bound micelles is observed.

Our results can be interpreted by assuming a necklace model for micelle adsorption, as indicated in Figure 8. Other models, such as the flexible rod one,³⁵ are not satisfactory from a dielectric viewpoint. In the latter hypothesis, for instance, the

occurrence of relaxation processes at frequencies above 100 MHz is expected, in disagreement with experiments.

The present model can be extended to biochemically relevant systems; similar mechanisms, in fact, have been postulated in systems containing proteins and surfactants or lipids. In the latter case, micelles adsorb onto the apolar region of the biomacromolecule, acting as junction points for the formation of interconnected protein–surfactant gels and other complex supramolecular aggregates.^{71,72}

Acknowledgment. Thanks are due to Dr. Carlo Sarnthein-Graf (Department Chemistry, La Sapienza) for help with the experimental work and Dr. Patrizia Cafarelli and Dr. Carla Ferragina, IMIP-CNR (Montelibretti), for supporting us in the synthetic procedures and material preparation. Part of the work presented here has been presented by P.M., in partial fulfillment of his graduate thesis, Rome, 2002. MIUR, the Ministry of University and Research Activities, is acknowledged for financial support, through a Cofin 2002–2004 project on Polymer–Surfactant Systems. Part of the present research work was performed under the auspices of COST D15 Project (2000–2004) on Interfacial Chemistry and Catalysis. We wish to acknowledge an anonymous reviewer for useful and exhaustive information on literature findings.

References and Notes

- (1) Macknight, W. J.; Ponomarenko, E. A.; Tirrell, D. A. *Acc. Chem. Res.* **1998**, *31*, 781.
- (2) Antonietti, M.; Conrad, J.; Thünemann, A. *Macromolecules* **1994**, *27*, 6007.
- (3) Goddard, E. D. *Colloids Surf.* **1986**, *19*, 255.
- (4) Goddard, E. D. *Colloids Surf.* **1986**, *19*, 301.
- (5) Goddard, E. D. In *Interactions of Surfactants with Polymers and Proteins*; Goddard, E. D., Ananthapadmanabhan, K. P., Eds; CRC Press: Boca Raton, 1993, p 395.
- (6) Shirahama, K. In *Polymer-Surfactant Systems*; Kwak, J. C. T., Ed.; Marcel Dekker: New York, 1998; Chapter IV, p 143.
- (7) Mel'nikov, S. M.; Dias, R.; Mel'nikova, Y. S.; Marques, E. F.; Miguel, M. G.; Lindman, B. *FEBS Lett.* **1999**, *453*, 113.
- (8) Brown, V. C. H. *J. Soc. Cosm. Chem.* **1971**, *22*, 411.
- (9) Shirahama, K.; Ide, N. *J. Colloid Interface Sci.* **1976**, *54*, 450.
- (10) Cabane, B. *J. Phys. Chem.* **1977**, *81*, 1639.
- (11) Harrison, I. M.; Candau, F.; Zana, R. *Colloid Polym. Sci.* **1999**, *277*, 48.
- (12) Thalberg, K.; Lindman, B.; Karlstrom, G. *J. Phys. Chem.* **1990**, *94*, 4289.
- (13) Bakeev, K. N.; Shu, Y. M.; MacKnight, W. J.; Zezzin, A. B.; Kabanov, V. A. *Macromolecules* **1994**, *27*, 300.
- (14) Sesta, B.; Segre, A. L.; D'Aprano, A.; Proietti, N. *J. Phys. Chem.* **1997**, *101*, 170.
- (15) La Mesa, C. *Colloids Surf., A* **1999**, *160*, 37.
- (16) Li, H.; Yu, G.-E.; Price, C.; Booth, C.; Hecht, E.; Hoffmann, H. *Macromolecules* **1997**, *30*, 1347.
- (17) Valstar, A.; Vasilescu, M.; Vigouroux, C.; Stilbs, P.; Almgren, M. *Langmuir* **2001**, *17*, 3208.
- (18) Holmberg, A.; Piculell, L.; Nyden, M. *J. Phys. Chem. B* **2002**, *106*, 2533.
- (19) Shtykova, E.; Dembo, A.; Makhaeva, E.; Khokhlov, A.; Evmenenko, G.; Reynaers, H. *Langmuir* **2000**, *16*, 5284.
- (20) Thuresson, K.; Nilsson, S.; Kjoniksen, A. L.; Walderhaug, H.; Lindman, B.; Nystroem, B. *J. Phys. Chem. B* **1999**, *103*, 1425.
- (21) De Lisi, R.; De Simone, D.; Milioto, S. *J. Phys. Chem. B* **2000**, *104*, 12130.
- (22) Proietti, N.; Amato, M. E.; Masci, G.; Segre, A. L. *Macromolecules* **2002**, *35*, 4365.
- (23) Shirahama, K.; Nagao, S. *Colloids Surf.* **1992**, *66*, 275.
- (24) Abuin, E. B.; Scajano, J. C. *J. Am. Chem. Soc.* **1984**, *106*, 6274.
- (25) Antonietti, M.; Foerster, S.; Zisenis, M.; Conrad, J. *Macromolecules* **1995**, *28*, 2270.
- (26) Antonietti, M.; Neese, M.; Blum, G.; Kremer, F. *Langmuir* **1996**, *12*, 4436.
- (27) Antonietti, M.; Maskos, M.; Kremer, F.; Blum, G. *Acta Polym.* **1996**, *47*, 460.
- (28) Sokolov, E.; Yeh, F.; Khokhlov, A.; Grinberg, V. Y.; Chu, B. *J. Phys. Chem. B* **1998**, *102*, 7091.

- (29) Zhou, S.; Yeh, F.; Burger, C.; Chu, B. *J. Phys. Chem. B* **1999**, 103, 2107.
- (30) Michiotti, P. M.S. Thesis, La Sapienza University, Rome, Italy, 2002.
- (31) Michiotti, P.; Cafarelli, P.; Ferragina, C.; La Mesa, C. *Chem. Eng. Trans.* 2003, 3, 1301.
- (32) Michiotti, P.; Bonicelli, M. G.; Cafarelli, P.; Ceccaroni, G. F.; Ferragina, C.; La Mesa, C. *Colloid Polym. Sci.* **2003**, 281, 431–438.
- (33) Antonietti, M.; Burger, C.; Effing, J. *Adv. Mater.* **1995**, 7, 751.
- (34) Wenzel, A.; Antonietti, M. *Adv. Mater.* **1997**, 9, 487.
- (35) Lundhal, P.; Greijer, E.; Sandberg, M.; Cardell, S.; Eriksson, K. *O. Biochim. Biophys. Acta* **1986**, 873, 20.
- (36) Benkhira, A.; Franta, E.; Francois, J. *J. Colloid Interface Sci.* **1994**, 164, 428.
- (37) Guo, X. H.; Zhao, N. M.; Chen, S. H.; Teixeira, J. *Biopolymers* **1990**, 29, 335.
- (38) Paredes, S.; Tribout, M.; Ferreira, J.; Leonis, J. *Colloid Polym. Sci.* **1976**, 254, 637.
- (39) La Mesa, C. *J. Phys. Chem.* **1990**, 94, 330.
- (40) Kogej, S. *J. Phys. Chem. B* **2003**, 107, 8003.
- (41) Wang, C.; Tam, K. C. *Langmuir* **2002**, 18, 6484.
- (42) *Handbook of Chemistry and Physics*, 74th ed.; CRC Press: Boca Raton, 1994; Tables 6–12.
- (43) Riddick, J. A.; Bunger, W. B.; Sakano, T. K. In *Techniques of Chemistry*, IVth ed.; Wiley: New York, 1986; Vol. II, p 263 and references therein.
- (44) Bonincontro, A.; Briganti, G.; Giansanti, A.; Pedone, F.; Risuleo, G. *Colloid Surf., B* **1996**, 6, 219.
- (45) Athey, T. W.; Stuckly, M. A.; Stuckly, S. S. *IEEE Trans. Microwave Theory Tech.* **1982**, 30, 82.
- (46) Barchini, R.; Pottel, R. *J. Phys. Chem.* **1994**, 98, 7899.
- (47) Shikata, T.; Imai, S. I. *Langmuir* **1998**, 14, 6804.
- (48) Imai, S. I.; Shikata, T. *Langmuir* **1999**, 15, 8388.
- (49) Baar, C.; Buchner, R.; Kunz, W. *J. Phys. Chem. B* **2001**, 105, 2906.
- (50) Imai, S. I.; Shiokawa, M.; Shikata, T. *J. Phys. Chem. B* **2001**, 105, 4495.
- (51) Penafiel, L. M.; Litovitz, T. A. *J. Chem. Phys.* **1992**, 97, 559.
- (52) Bordin, F.; Cametti, C.; Gili, T.; Colby, R. H. *Langmuir* **2002**, 18, 6404.
- (53) Mandel, M. *Ann. N.Y. Acad. Sci.* **1977**, 303, 74.
- (54) Mandel, M. *Biophys. Chem.* **2000**, 85, 125.
- (55) Gracida, A.; Creux, P.; Lachaise, J.; Salager, J. L. *Ind. Eng. Chem. Res.* **2000**, 39, 2677.
- (56) Khan, A.; Marques, E. F. *Curr. Opin. Colloid Interface Sci.* **1999**, 4, 402.
- (57) Marques, E. F.; Regev, O.; Khan, A.; da Graca Miguel, M.; Lindman, B. *J. Phys. Chem. B* **1999**, 103, 8353.
- (58) Grosse, C.; Foster, K. *J. Phys. Chem.* **1987**, 91, 6415.
- (59) Grosse, C. *J. Phys. Chem.* **1988**, 92, 3905.
- (60) Lobo, V. M. M.; Quaresma, J. L. *Handbook of Electrolyte Solutions*; Phys. Sci. Data Series 4; Elsevier: Amsterdam, 1989.
- (61) Gray, D. E. *American Institute of Physics Handbook*; McGraw-Hill: New York, 1972; pp 2–226.
- (62) Douh ret, G.; Viallard, A. *J. Chim. Phys.* **1981**, 78, 85.
- (63) *Physico-Chemical Properties of Selected Anionic, Cationic and Nonionic Surfactants*; Van Os, N. M., Haak, R., Rupert, L. A. M., Eds.; Elsevier: Amsterdam, 1993.
- (64) Hiemenz, P. C. *Principles of Colloid and Surface Chemistry*; Marcel Dekker: New York, 1986; Chapter XII, p 691.
- (65) Muzzalupo, R.; Ranieri, G. A.; La Mesa, C. *Colloids Surf., A* **1995**, 104, 327.
- (66) Durand-Vidal, S.; Turq, P.; Bernard, O.; Treiner, C. *J. Phys. Chem. B* **1997**, 101, 1713.
- (67) Chang, J. N.; Kaler, E. W. *J. Phys. Chem.* **1985**, 89, 2996.
- (68) Zana, R. *J. Colloid Interface Sci.* **1980**, 70, 330.
- (69) Caponetti, E.; Triolo, R.; Ho, P. C.; Johnson, J. S.; Magid, L. J.; Butler, P.; Payne, K. A. *J. Colloid Interface Sci.* **1987**, 116, 200.
- (70) Mandel, M.; Odijk, T. *Annu. Rev. Phys. Chem.* **1984**, 35, 75.
- (71) Moren, A. K.; Regev, O.; Khan, A. *J. Colloid Interface Sci.* **2000**, 222, 170.
- (72) Sesta, B.; Capalbi, A.; Gente, G.; Iovino, A.; La Mesa, C.; Laureti, F.; Michiotti, P.; Paiusco, O.; Palacios, A. C.; Persi, L.; Princi, A.; Sallustio, S.; Sarnthein-Graf, C. *J. Phys. Chem.*, submitted for publication.